Electronic supplementary information for

Fluoride-Bridged Dinuclear Dysprosium Complex Showing Single Molecule Magnetic Behavior: Supramolecular Approach to Isolate Magnetic Molecules

Dong-fang Wu, Kiyonori Takahashi,* Masaru Fujibayashi, Naoto Tsuchiya, Goulven Cosquer, Rui-Kang Huang, Chen Xue, Sadafumi Nishihara, Takayoshi Nakamura*

Table of Contents

§1. Single crystal X-ray analysis

Table S1. Crystallographic and structure refinements for Crystal **1**.

Crystal	**1**
Formula	$C_{160}H_{291}Dy_2Na_{10}O_{163.5}F_2P_2W_{22}$
Molecular weight/g mol^{-1}	9530.23
Crystal system	triclinic
space group	*P*
a/Å	17.5657(6)
b/Å	17.8718(6)
c/Å	24.6678(7)
α/deg	83.624(3)
β/deg	78.593(3)
γ/deg	66.807(3)
V / Å^3	6972.8(4)
Z	1
T / K	98
ρ_{calc} / g cm^{-3}	2.108
μ / mm^{-1}	20.085
F(000)	4085.0
2θ / ^{o}	5.384 to 145.12
Reflections collected	81221
Independent reflections	26470
Data / restraints / param	26470/517/1508
R_{int}	0.0440
R_1 [I > 2σ(I)]	0.0824
wR_2 (all data)	0.2706
GOF on F^2	1.035
$\Delta\rho_{max/min}$/e Å^{-3}	3.471/-1.704

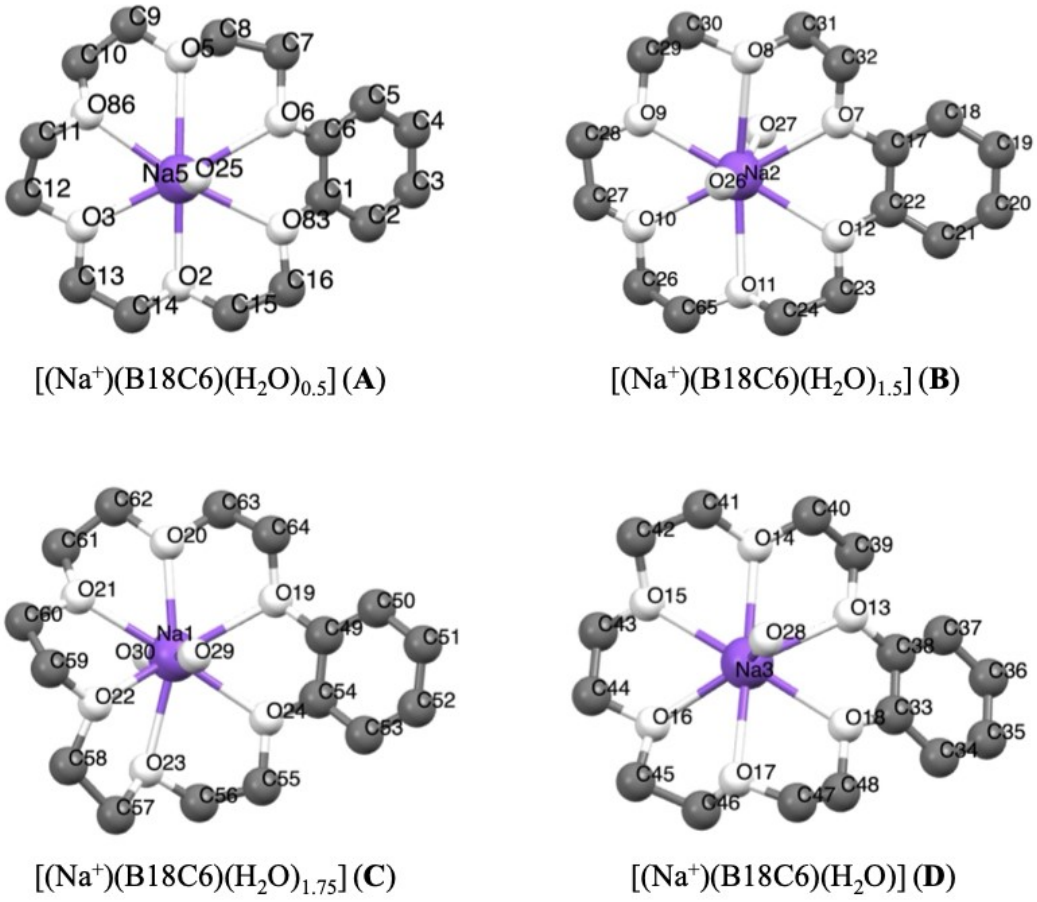

Figure S1. Crystallographically independent structure of (Na)(B18C6) units (**A**, **B**, **C**, and **D**) in crystal **1** at 94 K. Hydrogen atoms are omitted for clarity. Gray, white and purple atoms correspond to carbon, oxygen and sodium, respectively.

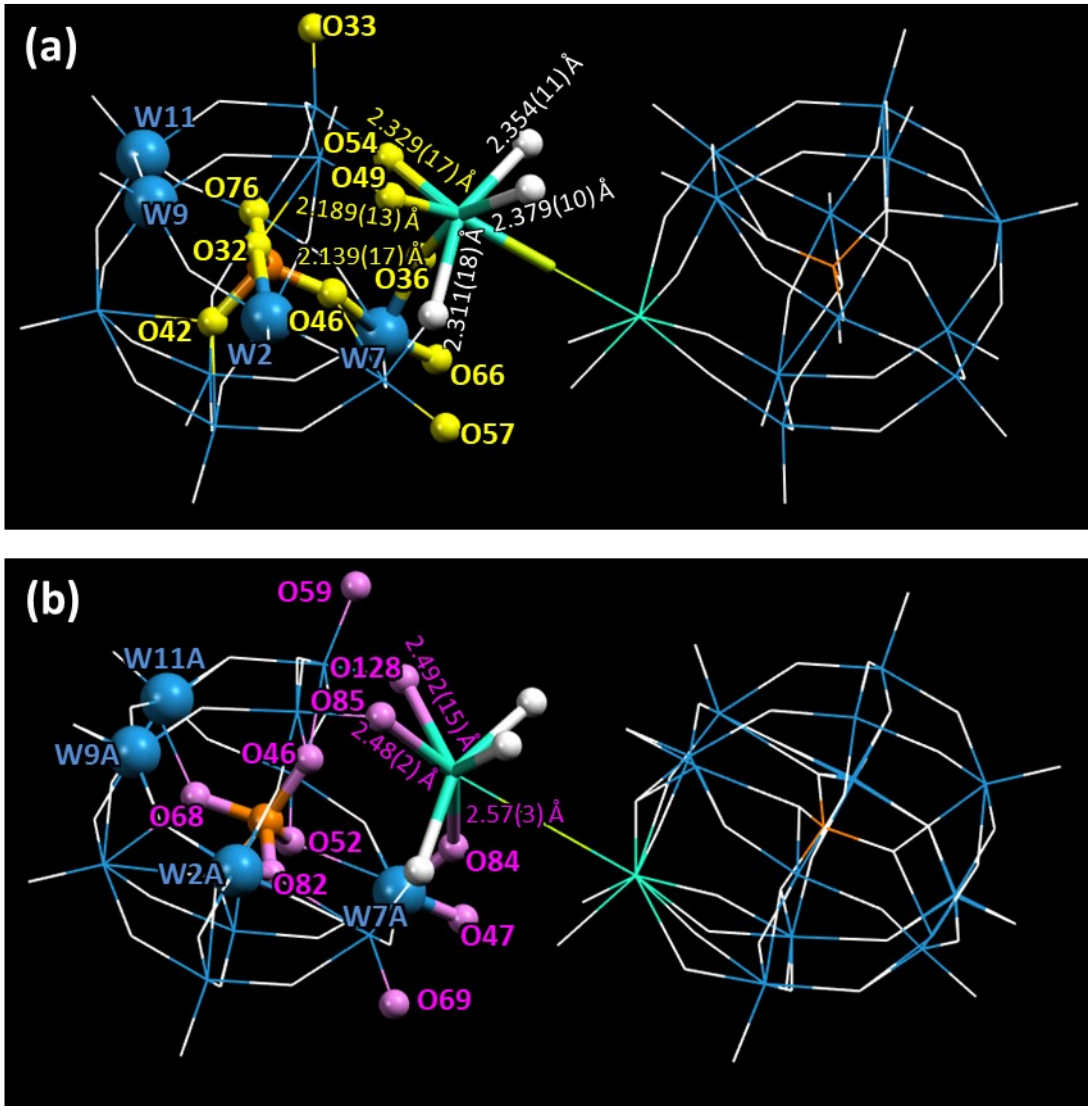

Figure S2. Disordered structure of $\{[(PW_{11}O_{39})Dy(H_2O)_2)]F\}^{9-}$ anion in crystal **1** at 94 K with atoms which are with occupancies of (a) 0.566(8) and (b) 0.444(8), respectively. Hydrogen atoms are omitted for clarity. Color code is as same as that in Figure 1 except O atoms at disordered sites. Dy-O distances are shown in the figures.

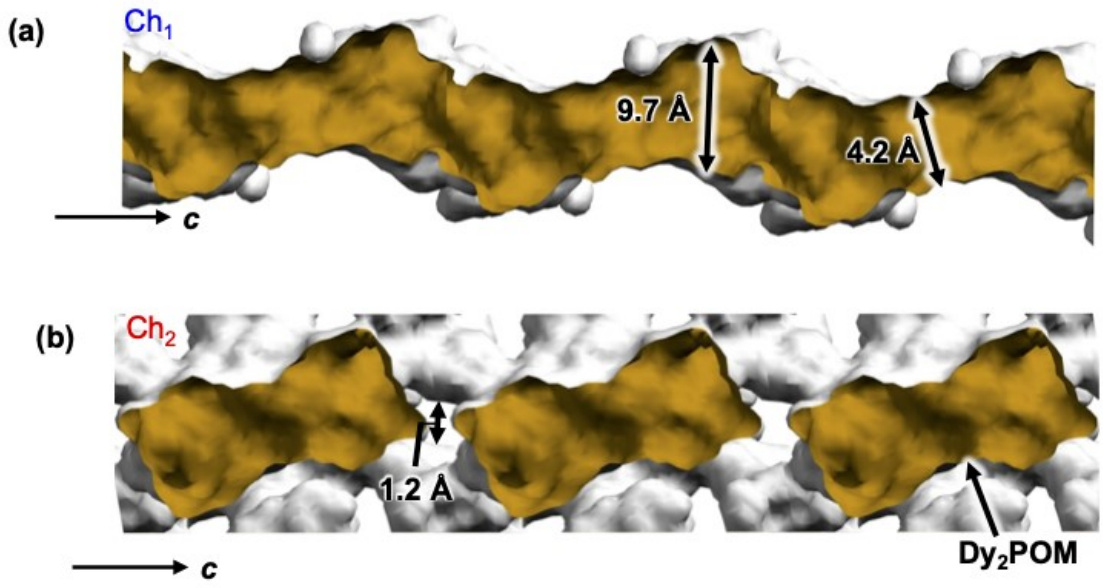

Figure S3. One-dimensional channel structures of (a) Ch_1 and (b) Ch_2 along the *c*-axis, displayed using the void function of Mercury software. The inner wall of the channel vacancy is shown in yellow and the outer wall in white. To display the Ch_1 and Ch_2, uncoordinated crystalline H_2O molecules and Dy_2POM are removed from the structure, respectively. The distances shown are the center-to-center distances of the corresponding terminal atoms minus the van der Waals radii.

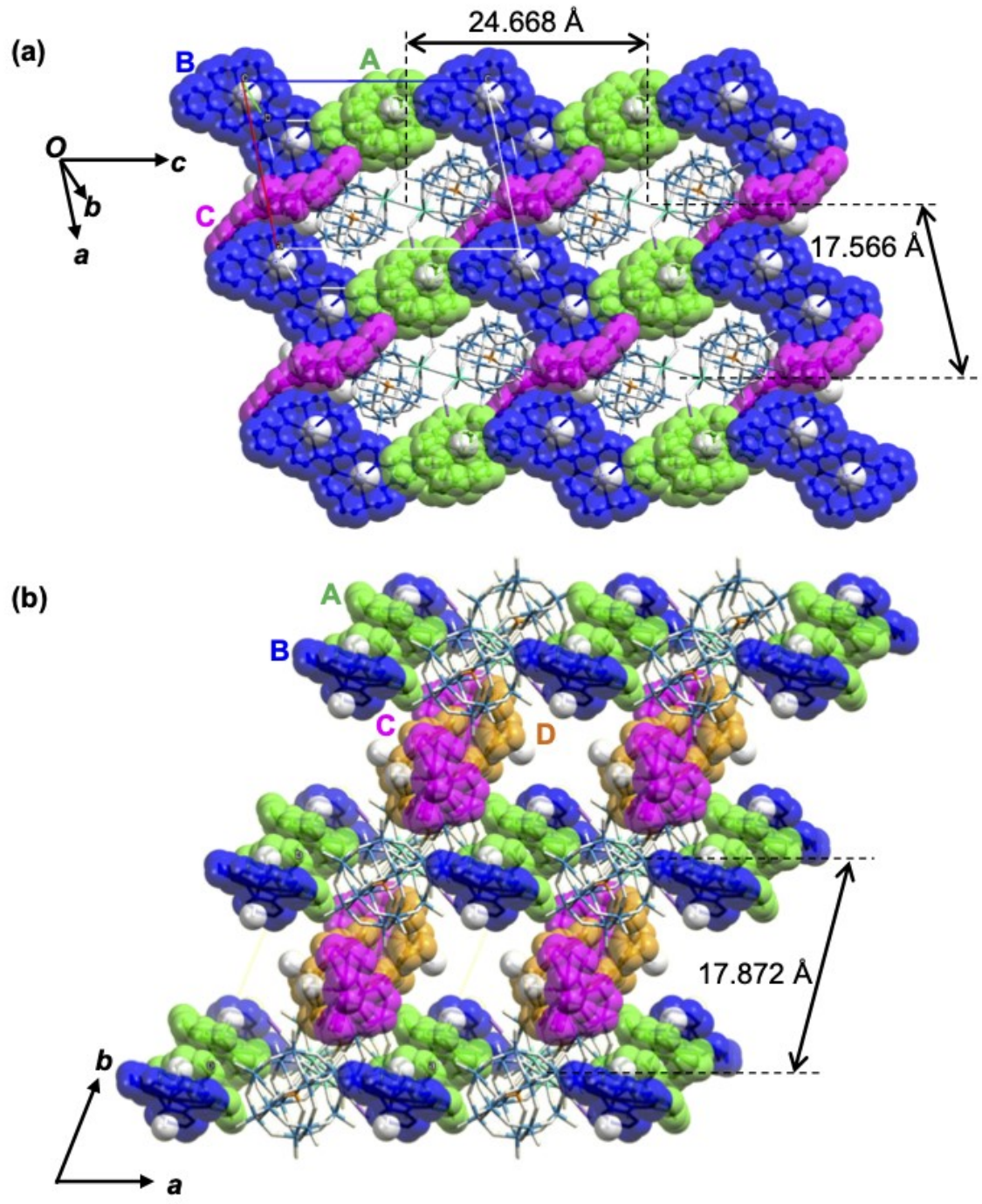

Figure S4. Packing structure of crystal **1** viewed along the (a) *b* and (b) *c* axes. The central F^- distances between adjacent Dy_2POMs are given in the figure.

§1. X-ray photoelectron spectroscopy

X-ray photoelectron spectroscopy (XPS) data were collected on a JPS-9200 X-ray photoelectron spectrometer, using monochromatic Al Kα radiations (hν = 1486.6 eV).

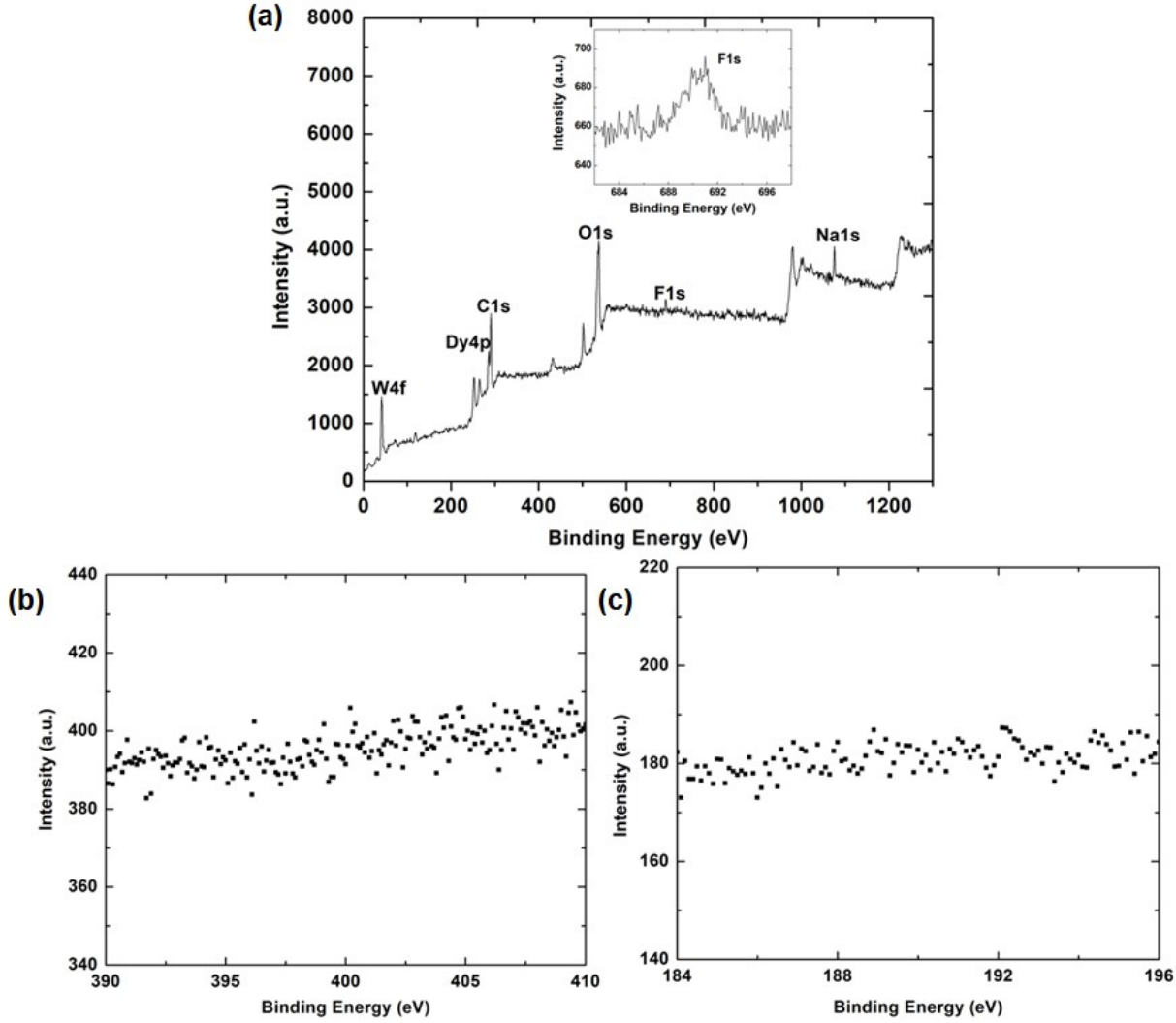

Figure S5. XPS spectra of crystal **1**. (a) survey scan, Inset: the core level spectrum of F 1s, (b) the core level scan for N 1s, (c) the core level scan for B 1s.

§2. Scanning electron microscopy (SEM) and energy dispersive X-ray spectroscopy (EDS)

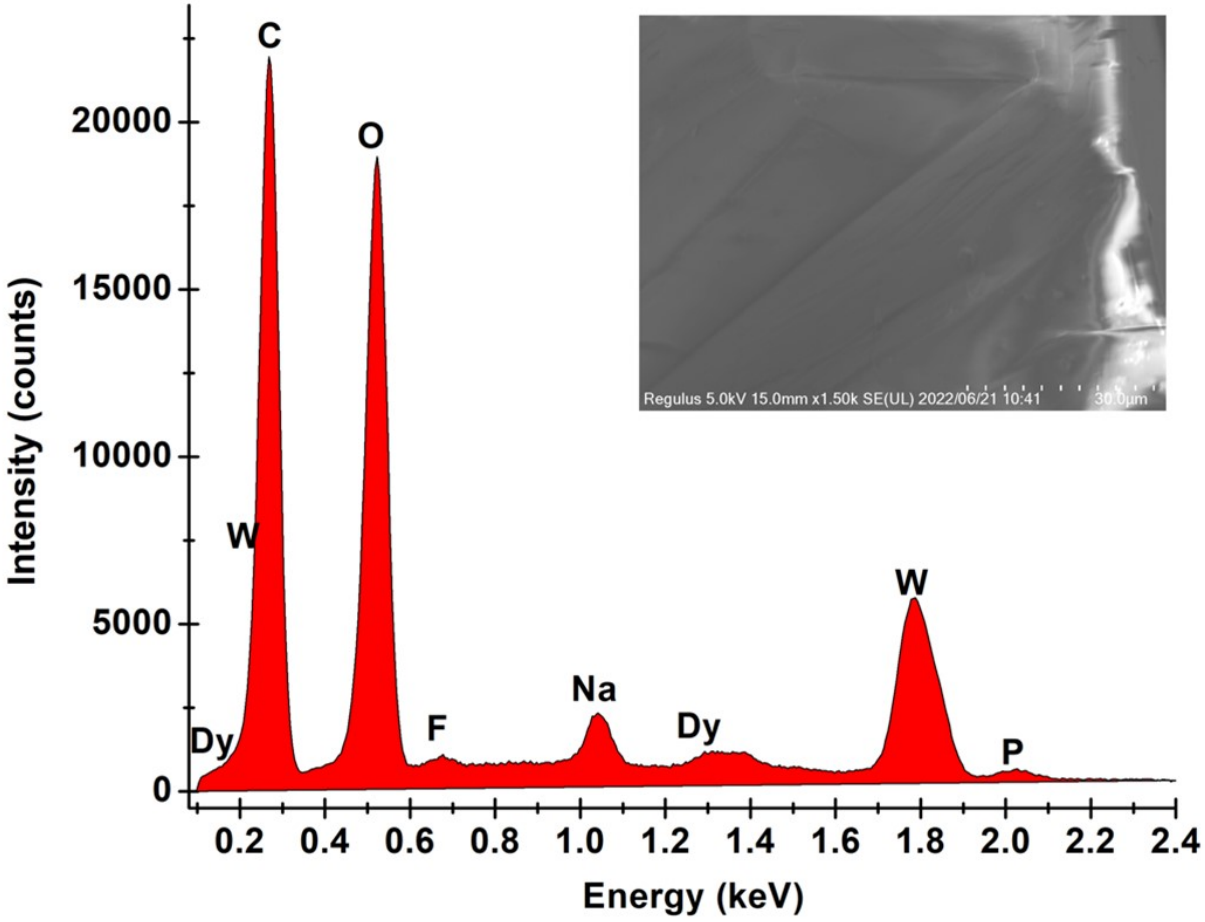

Figure S6. The EDS spectrum of crystal **1**. Inset left: magnified SEM image of view of crystal **1**.

Table S2. Elemental composition results of crystal **1**.

Element	Mass (%)	Mass Norm. (%)	Atom (%)	abs. error (%) (1 sigma)
C	**17.92**	**24.87**	**49.24**	**1.98**
O	**21.19**	**28.02**	**41.65**	**2.22**
F	**0.27**	**0.38**	**0.48**	**0.07**
Na	**1.71**	**2.37**	**2.46**	**0.12**
P	**0.46**	**0.63**	**0.49**	**0.05**
W	**30.20**	**41.92**	**5.42**	**1.43**
Dy	**1.30**	**1.80**	**0.26**	**0.10**
	96.20	**100.00**	**100.00**	

When the acceleration voltage is fixed, it is generally difficult to quantify atoms that are far apart in atomic number, because the electron diffusion region becomes smaller as the atomic number increases. Therefore, only F, Na, and P with close atomic numbers were compared. Conductive carbon tape was used to fix the sample, therefore the comparison of carbon and oxygen contents are not applied.[S1]

§3. Thermogravimetric Analyses (TGA)

The amount of H_2O in the crystals is difficult to determine accurately because the TGA curve includes desorption of other molecules. Since the desorption curve is nearly linear from 100 to 180 °C, it is assumed that desorption of water molecules ends at 180 °C. The weight loss of 5.2 wt% at 180 °C corresponds to about 28 molecules of H_2O per crystal composition.

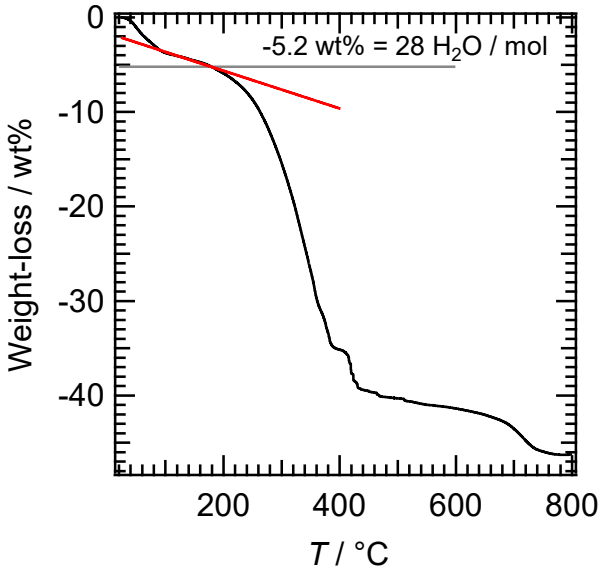

Figure S7. Thermogravimetric analysis of crystal **1**.

§5. Infrared Spectroscopy

The IR spectrum of crystal **1** is shown in the Figure S8. The band of 3645 cm^{-1} is attributed to the stretch of O-H bond. The band near 1118 cm^{-1} implied the C–O–C asymmetric stretching vibration of B[18]crown-6 molecule. Characteristic bands around 1594, 1503 and 1450 cm^{-1} are assigned to benzene ring stretch of B[18]crown-6 molecule. As for the bands at 700-1000 cm^{-1}, that is caused by the asymmetric stretch of the W–O_c–W (700–780 cm^{-1}) and W–O_b–W (880–910 cm^{-1}) bridges and of the W–O_d terminal bonds at around 940 cm^{-1} (O_d is a terminal oxygen, O_b is a bridging oxygen between corner-sharing octahedra, and O_c is a bridging oxygen between edge-sharing octahedra). A pair of characteristic bands at 1038 and 1070 cm^{-1} corresponding to the v_3 vibrational mode of PO_4 of A-type trivacant Keggin unit implies that the loss of local symmetry.[S2–S4]

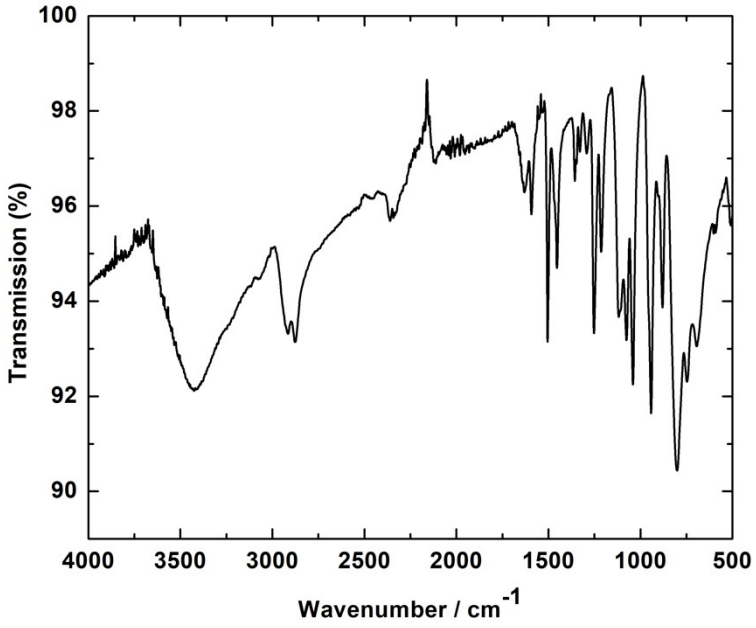

Figure S8. infrared spectrum of crystal **1**.

§6. Magnetic Properties

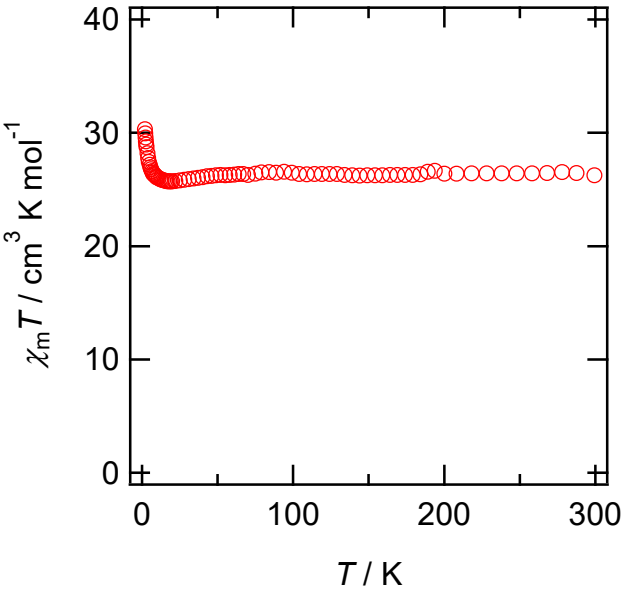

Figure S9. Temperature dependence of the product of molar magnetic susceptibility (χ_m) with temperature (T) of polycrystalline sample of **1**.

Debye model

$$\chi(\omega) = \chi_S + \frac{\chi_T - \chi_S}{1 + (i\omega\tau)^{(1-\alpha)}} \qquad \text{(S1)}^{S5}$$

(a) (b)

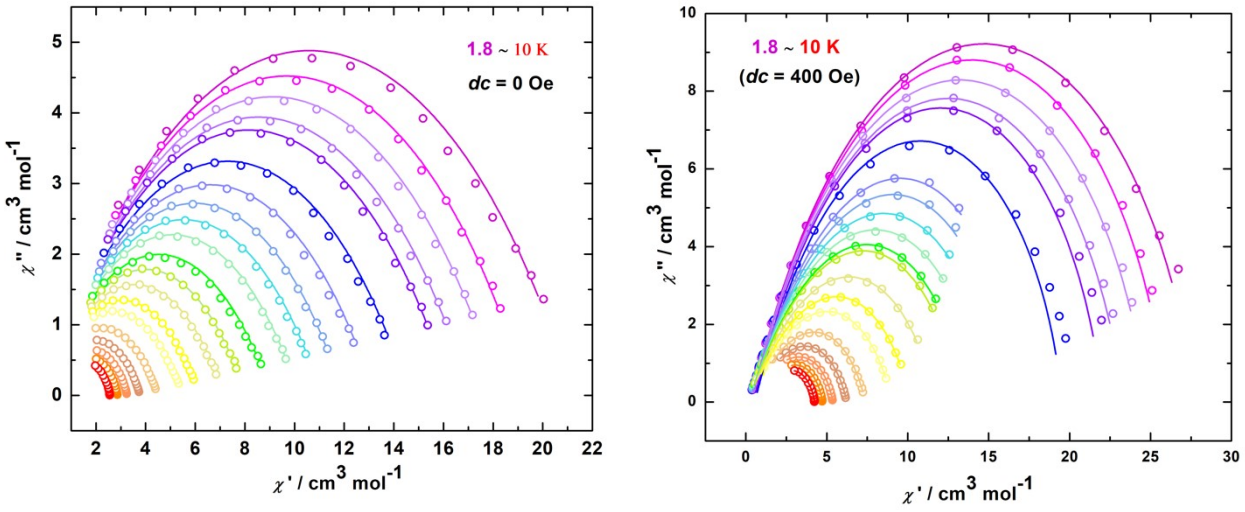

Figure S10. Cole−Cole plots for temperatures between 1.8−10 K under a zero (a) and 400 (b) *dc* field with the best fit to the single Debye model (Eq.S1) for crystal **1**. The Solid lines represent fits to the data.

Table S3. The best fitting parameters for Cole−Cole plots of compound **1** at varying temperatures under zero applied dc field.

T	χ_S	χ_T	α
1.8	0	21.192466	0.45035163
1.9	0	19.3937972	0.44446635
2	0	18.2442194	0.44742188
2.1	0	17.0863057	0.44985993
2.2	0	16.3184765	0.45059601
2.4	0	14.5864714	0.45686191
2.6	0	13.1960621	0.45946906
2.8	0	11.9462859	0.45576124
3	0	11.0758819	0.46236295
3.2	0	10.1693286	0.46430385
3.4	0	9.05940515	0.47166921
3.5	0	8.02227386	0.46693983
4	0	7.15589366	0.47337803
4.5	0	6.13996775	0.4739653
5	0	5.5714513	0.48668961
6	0.03073985	4.50138187	0.485899
7	0.32027434	3.7928435	0.46476434
8	0.66946806	3.27265807	0.42838084
9	0.90865253	2.88093638	0.38782117
10	1.02671352	2.56745008	0.34751153

Table S4. The best fitting parameters for Cole−Cole plots of compound **1** at varying temperatures under 400 Oe applied *dc* field.

T	χ_S	χ_T	α
1.8	0.47720395	28.477204	0.2633432
1.9	0.69298358	26.1929836	0.2337136
2	0.63435157	24.9343516	0.24015537
2.1	0.61247377	23.6124738	0.24373576
2.2	0.65285526	22.6528553	0.23941641
2.4	0.531479	20.531479	0.257792
2.6	0.44538531	18.4453853	0.28599004
2.8	0.44244205	17.442442	0.29620814
3	0.40297562	16.4029756	0.31354316
3.2	0.41549169	15.2154917	0.31935654
3.4	0.41065941	14.2106594	0.33015173
3.5	0.49149924	13.4914992	0.31846465
4	0.45522819	11.9552282	0.35379342
4.5	0.5754422	10.2754422	0.35112705
5	0.63509855	9.13509855	0.3608778
6	0.90417032	7.40417032	0.35140942
7	0.81421822	6.31421822	0.38144872
8	1.1274637	5.4274637	0.35959779
9	1.37139023	4.77139023	0.33849239
10	1.61126828	4.26126828	0.30040819

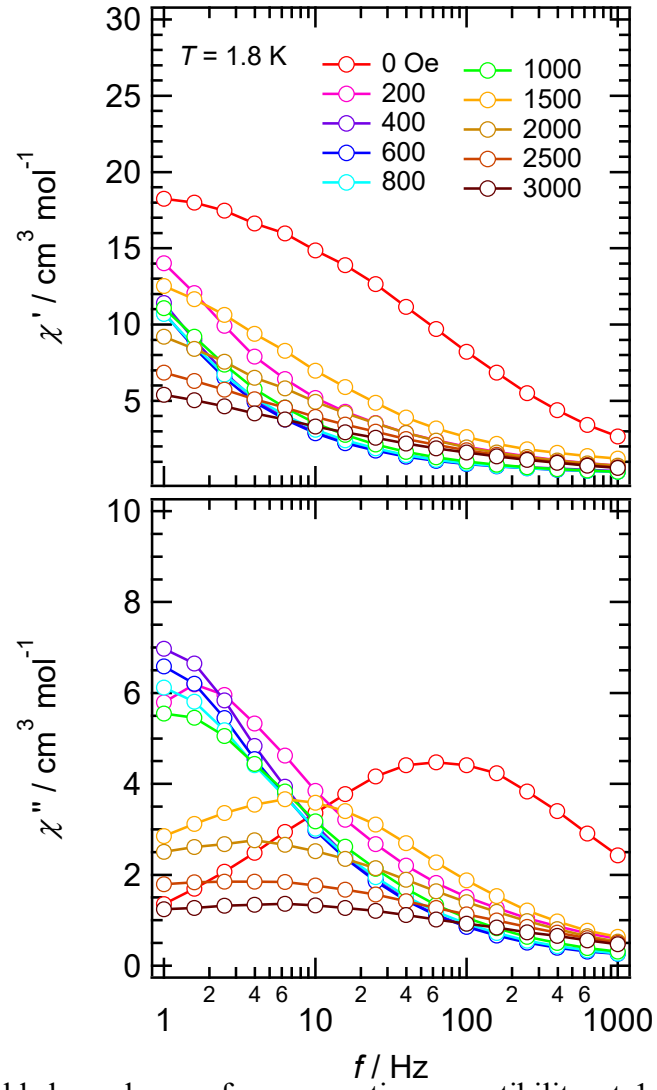

Figure S11. Field dependence of ac magnetic susceptibility at 1.8 K under the several direct magnetic fields from 0 to 3000 Oe. Lines are guided for eye.

References

S1 M. Abd Mutalib, M. A. Rahman, M. H. D. Othman, A. F. Ismail and J. Jaafar, in *Membrane characterization*, Elsevier, 2017, pp. 161–179.

S2 R. Khoshnavazi, F. Nicolò, H. A. Rudbari, E. Naseri and A. Aminipour, *Journal of Coordination Chemistry*, 2013, **66**, 1374–1383.

S3 V. Lahootun, C. Besson, R. Villanneau, F. Villain, L. M. Chamoreau, K. Boubekeur, S. Blanchard, R. Thouvenot and A. Proust, *J Am Chem Soc*, 2007, **129**, 7127–7135.

S4 T. Chatterjee, M. Sarma and S. K. Das, *Crystal Growth and Design*, 2010, **10**, 3149–3163.

S5 Y. N. Guo, G. F. Xu, Y. Guo and J. Tang, *Dalton Transactions*, 2011, **40**, 9953–9963.